ANALYSIS OF HOT WORKABILITY OF NICKEL-CHROMIUM ALLOY

ŁUKASZEK-SOŁEK Aneta[1], ŚWIĄTONIOWSKI Andrzej[2], CELADYN Krzysztof [2]

[1]AGH University of Science and Technology, Faculty of Metals Engineering and Industrial Computer Science, Cracow, Poland, EU

[2]AGH University of Science and Technology, Faculty of Mechanical Engineering and Robotics, Cracow, Poland, EU

Abstract

Nickel-chromium alloys are increasingly used in constructions of the most loaded machine components including aircraft engines. Therefore, determining the parameters of metal forming for those alloys is very important. The hot deformation behaviour of Ni55Cr45 alloy with cast starting structure was investigated in the temperature range of 750-1150 °C and strain rate range of 1-100 s^{-1}. The workability consists of two parts: the intrinsic workability and the State-of-Stress (SoS) workability. Processing maps showing the intrinsic workability dependent on material properties have been drawn on the basis of experimental data from compression tests carried out on a Gleeble 3800 thermomechanical simulator and based on the Prasad's approach. Due to the significant influence of strain on the efficiency of power dissipation parameter η and the instability parameter ξ, maps were drawn for a true strain in a range of 0.1-0.9. The processing windows and the flow instability regions have been determined. By using Lua scripts processing maps have been integrated with the commercial software based upon FEM - QForm V8 for numerical calculation, which made possible to designate the distribution of the flow instability parameter ξ during forging. In addition, the strain rate sensitivity parameter m and the efficiency of power dissipation parameter η for the investigated forgings have been determined. Such approach has allowed to integrate the intrinsic workability and the State-of-Stress workability and showed that it can be considered as an effective method of workability analysis.

Keywords: Ni55Cr45, processing maps, workability, State-of-Stress.

1. INTRODUCTION

Nickel and chromium superalloys are finding wider and wider application in constructing machines, devices and installations functioning under extremely difficult conditions [1]. The majority of products manufactured with the use of nickel and chromium alloys is obtained with the application of casting technologies. Over the recent years, however, a growing interest in increasing the mechanical properties of this type alloys by means of plastic deformation has been observed [2-5]. Unfortunately, the plastic deformation of that type alloys is restricted by the low level of the plastic properties of them, and the fact that they strengthen rapidly. In order to overcome the technological difficulties connected with the forming of NiCr alloys, the processing maps are useful [6-10]. The P-maps allow to determine the optimum range of temperature, strain rate, and the strain making it possible to obtain a forging free of defects of the material (structure) and/or of geometry (laps, folds, cracks). Optimum selected parameters will make it possible to obtain the appropriate degree of deformation of the material indispensable for the purpose of the reconstruction of internal crystal structure and obtaining required properties in entire volume [11]. The high heat resistance and high-temperature creep resistance is typical of NiCr alloys. The possibility of guaranteeing in deformation processes the narrowed ranges of size and shapes tolerance, results the wide application of the forgings and profiles in many innovative sectors of industry (the aviation industry, chemical industry, power industry, and also mining of petroleum and gas, including shale gas).

In this paper, the hot deformation behaviour of the Ni55Cr45 alloy having the crystal structure in the process of upset forging was investigated. The processing maps based upon the Prasad's approach were drawn to

determine the optimum conditions of the hot working processes. Moreover, the influence of strain upon the processing maps was analyzed, in terms of the location, size and shape of the flow instability area. The processing maps were integrated with the commercial software based upon FEM for the simulations of forging processes, QForm V8. The distributions of the workability parameters were determined, including the identification of places where flow instability occurs.

2. MATERIALS AND EXPERIMENTS

The chemical composition of the Ni55Cr45 alloy is given in **Table 1**. The material was supplied as a cast bar. For developing processing maps, cylindrical samples (∅10 x 12 mm) were machined from the alloy. The compression tests were conducted on a Gleeble 3800 thermo-simulator. The research was conducted over the temperature range of 750-1150 °C and the strain rate range of 1-100 s^{-1} up to the constant true strain value of 0.9. The inverse method was applied for the interpretation of the results obtained from axisymmetric compression tests.

Table 1 Chemical composition (% weight) of the Ni55Cr45 alloy

Ni	Cr	Fe	Mn	Mo	N	C	P	S	Si
54.80	44.00	1.00	0.05	0.003	0.01	0.012	0.003	0.007	0.115

3. PROCESSING MAPS

The results of compression test were used for plotting of processing maps. The construction of processing maps based on Dynamic Material Modelling was described in many publication [6-10, 12-13]. In order to describe the hot deformation behaviour of investigated alloy some workability parameters are calculated. The strain rate sensitivity parameter m can be determined from

$$m = \frac{\partial \log \sigma}{\partial \log \dot{\varepsilon}} \tag{1}$$

The efficiency of power dissipation parameter η can be expressed as

$$\eta = \frac{2m}{m+1} \tag{2}$$

Power dissipation maps as the function of temperature and strain rate were plotted in the form of the isoclines of the power dissipation efficiency parameter expressed in %. The instability criterion (Eq. 3) was used to identify the regimes of unstable flow and to plot the instability maps in the frame of deformation temperature and strain rate. The instability criterion can be written as

$$\xi(\dot{\varepsilon}) = \frac{\partial \log\left(\frac{\mathrm{m}}{\mathrm{m}+1}\right)}{\partial \log \dot{\varepsilon}} + \mathrm{m} \leq 0 \tag{3}$$

By superimposing a flow instability map on a power dissipation map processing maps are created. **Fig. 1** shows the created processing maps at the temperature range of 750-1150 °C and the strain rate range of 1-100 s^{-1} for the true strains of 0.1, 0.3, 0.5 and 0.9. The efficiency of power dissipation parameter η is shown in the form of isocline (expressed in %), whereas the shaded regions indicate 'unsafe' areas in the processing map.

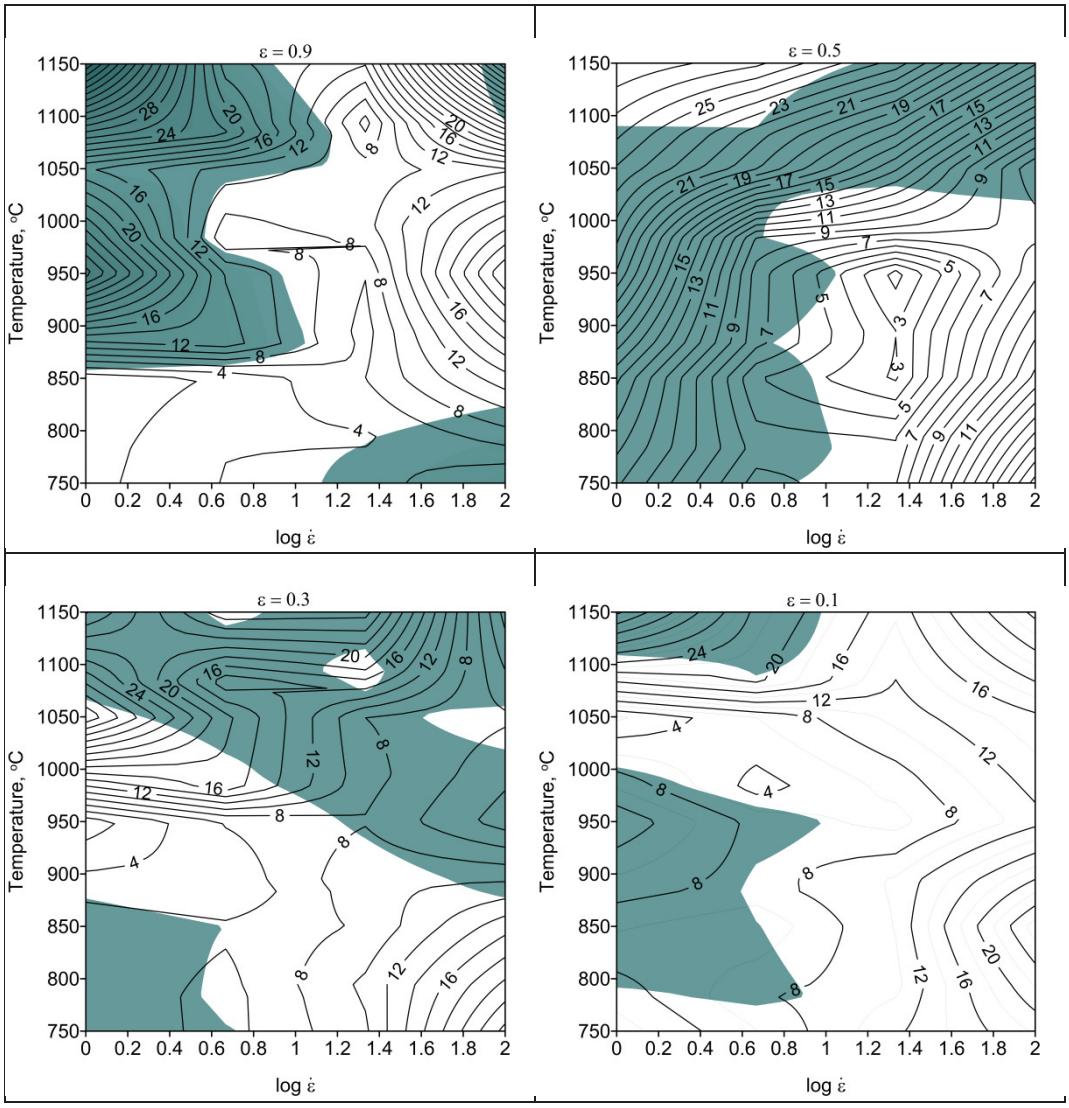

Fig. 1 The processing maps of Ni55Cr45 alloy at different true strains.
The shaded areas indicate the flow instability

4. NUMERICAL MODELLING

The numerical modelling of the isothermal forging process of Ni55Cr45 alloy was conducted in a commercial software based on FEM - QForm V8 [14]. By means of user subroutines (LUA scripts), the processing maps according to Prasad's approach were integrated into QForm V8. The numerical distribution of the strain rate sensitivity parameter m, the efficiency of power dissipation parameter η and flow instability parameter ξ were determined. The dimensions of the sample, the forging parameters such temperature and deformation velocity (strain rate too) was the same like during compression tests. Forging process was carried out at isothermal conditions. The temperature and strain rate (corresponding to the peak of the efficiency of power dissipation η) are determined on the basis of the processing map for true strain 0.9 and adopt T = 950 °C and $\dot{\varepsilon}$ = 100 s^{-1}. One-operation forging process was conducted on screw press of the nominal energy and nominal load at the level of 0.8 kJ and 0.4 MN respectively. The maximum speed of the press ram at the moment of contact of the tool with the workpiece was set at 600 mm / s. In **Figs. 2 - 4** the numerical distributions of workability parameters in characteristic cross-sections of the forgings at different strains are shown.

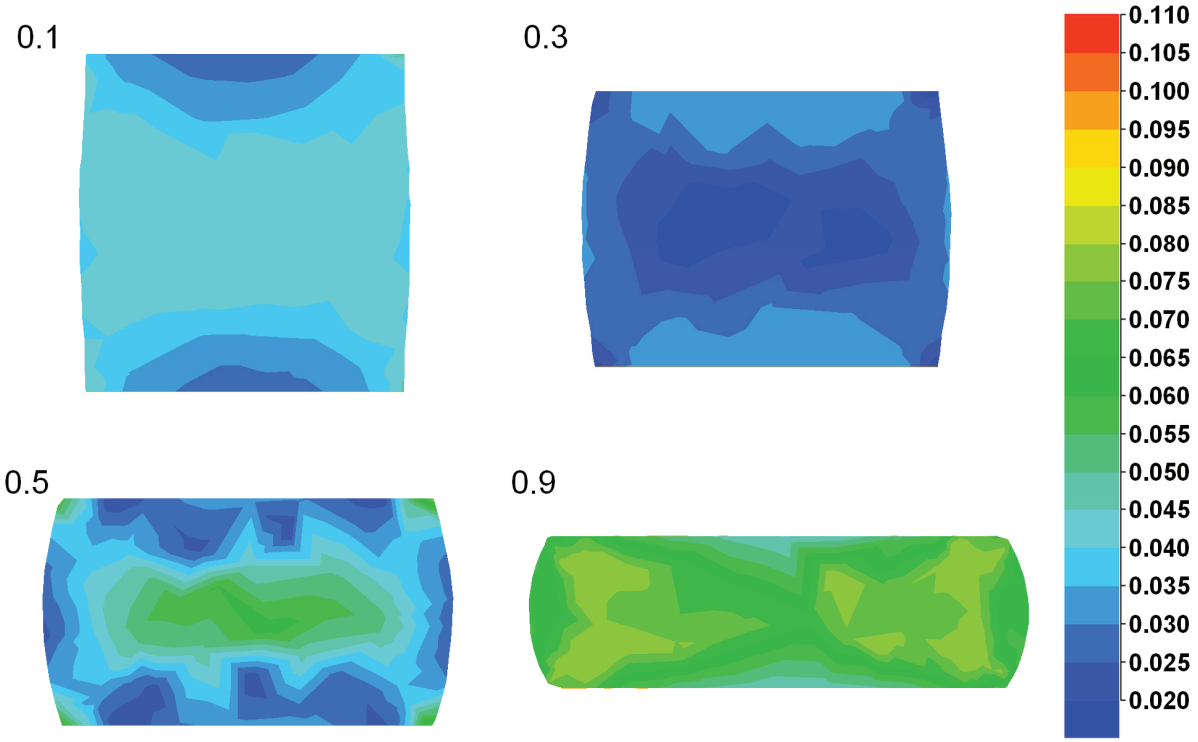

Fig. 2 Numerical distributions of the strain rate sensitivity parameter *m* for different values of true strain

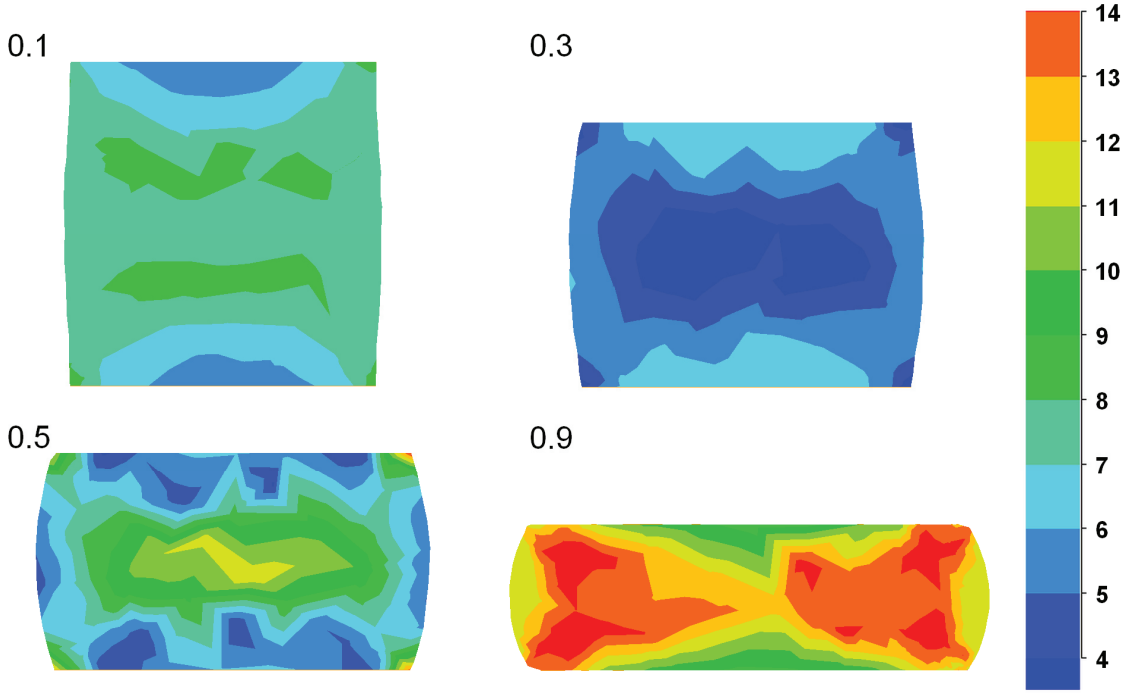

Fig. 3 Numerical distributions of the efficiency of power dissipation parameter η for different values of true strain

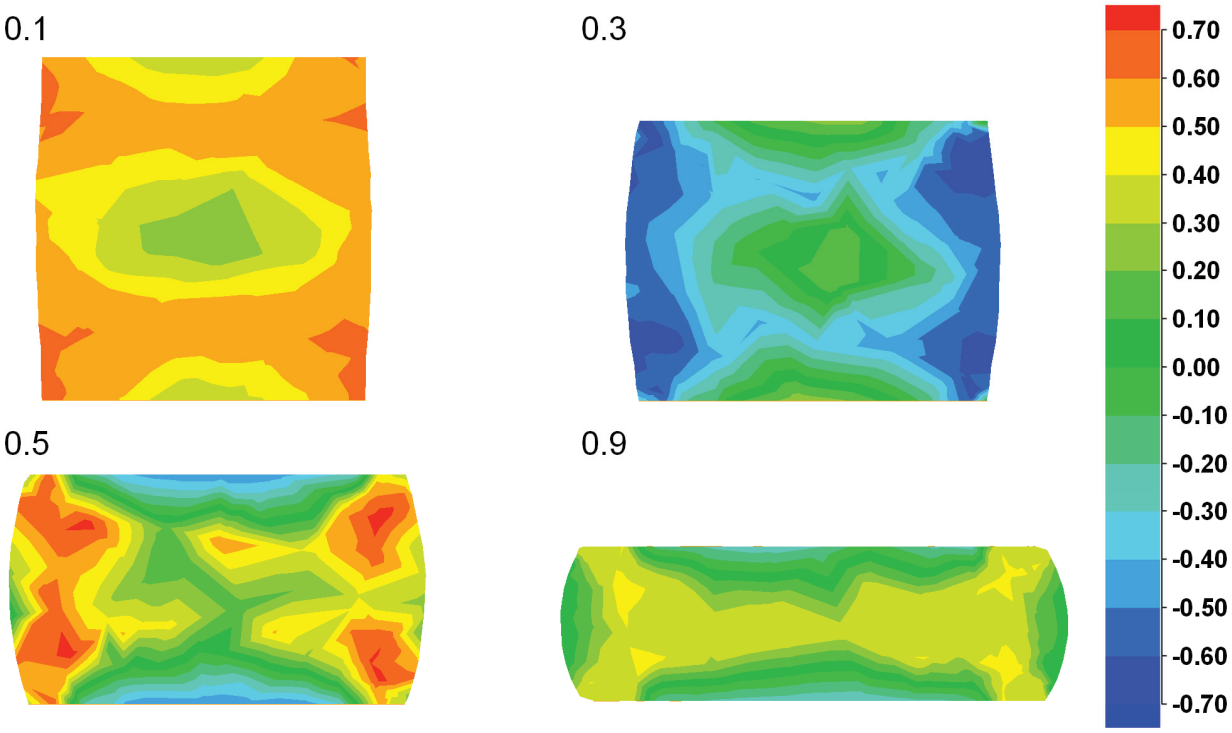

Fig. 4 Numerical distributions of the flow instability parameter ξ for different values of true strain

5. RESULTS AND DISCUSSION

On the processing maps (**Fig. 1**) can be observed the effect of true strain on the efficiency of power dissipation η and the instability areas. The flow instability areas, together with decreasing true strain vary their location, size and shape. The efficiency of power dissipation parameter η is sensitive to strain, temperature and strain rate. The high values of the parameter η, located in the ′unsafe′ areas, are most likely to be connected in this case with negative phenomena occurring in the microstructure. Such a situation may occur in the case of materials having casting structure (not worked), as well as those not subjected to heat treating. On the processing map for the true strain of 0.9, three flow instability areas were separated; these may cause the occurrence in the microstructure of the following: local voids, slip bands, shear bands, adiabatic shear bands and/or small cracks inside a forging, as well as on the surface of it. On the processing map, it is also possible to identify two domains for true strain of 0.9, which can fulfil a purpose of processing windows. For the temperature of 950 °C, and also strain rate of 100 s^{-1}, a peak of the efficiency of power dissipation η reaching 26 % occurs. It is possible to separate the processing window, limited by the isocline of the parameter η of the value of 16 % (i.e. described, approximately, by the following range: temperature: 875-1025 °C and strain rate of 40-100 s^{-1}). The other processing window may be determined for the range of temperature of 1075-1150 °C and the strain rate of 25-65 s^{-1}. The numerical distribution of workability parameters at strains of 0.1, 0.3, 0.5 and 0.9 is shown in **Figs. 2-4**. The strain rate sensitivity parameter m and the efficiency of power dissipation parameter η vary with increasing strain. Both of parameters increase with increasing strain. The numerical distribution of flow instability parameter ξ at different true strains indicates the regions of unstable flow ($\xi \leq 0$). The flow instability regions narrow with increasing strain and locate in the contact region of material and tools. In this area, there may be microstructural defects.

6. CONCLUSION

The hot deformation behaviour of the Ni55Cr45 alloy was investigated in the wide ranges of forming temperature and strain rate. The processing maps vary with increasing strain. The processing map at the true strain of 0.9 exhibits two processing windows, which allow to determine the optimum parameters for the investigated alloy, whereas, the processing maps were integrated into the commercial program QForm V8 based upon FEM by using the specially-written LUA scripts. Upon the basis of the results of numerical simulations of the investigated forging process, the optimal technological parameters of forging the Ni55Cr45 alloy were determined.

ACKNOWLEDGEMENTS

The research project was financed by the Ministry of Science and Higher Education (AGH-UST statutory research project no. 11.11.130.957).

REFERENCES

[1] ŚWIĄTONIOWSKI A., SIŃCZAK J., ŁUKASZEK-SOŁEK A., SCHMIDT J. Analysis of forging process of the NiCrN superalloy for motor boat driving shaft. Archives of Metallurgy and Materials, Vol. 57, No. 3, 2012, pp.719-725.

[2] WANG J., DONG J., ZHANG M., XIE X.: Hot working characteristics of nickel-base superalloy 740H during compression. Materials Science and Engineering: A, Vol. 566, 2013, pp. 61-70.

[3] BROOKS J.W.: Forging of superalloys. Materials and Design, Vol. 21, No. 4, 2000, pp. 297-303.

[4] DAYONG C., LIANGYIN X., WENCHANG L., GUIDONG S., MEI Y. Characterization of hot deformation behavior of Ni-base superalloy using processing map. Materials and Design, Vol. 30, No. 3, 2009, pp. 921-925.

[5] BARIANI P.F., BRUSCHI S., DAL NEGRO T. Prediction of nickel base superalloys rheological behavior under hot forging conditions using artificial neural networks. Journal of Materials Processing Technology, Vol. 152, No. 3, 2004, pp. 395-400.

[6] PRASAD Y.V.R.K., SASIDHARA S. Hot working guide: A compendium of processing maps, ASM International. Materials Park: Ohio, 1997.

[7] PRASAD Y. V. R. K. Processing maps: A status report. Journal of Materials Engineering and Performance, Vol. 12, No. 6, 2003, pp. 638-645.

[8] ŁUKASZEK-SOŁEK A., Technological aspect of processing maps for the AA2099 alloy, Acta Metallurgica Sinica (English Letters), Vol. 28, No. 1, 2015, pp. 22-31.

[9] LUO J., LI M., YU W., LI H., Effect of the strain on processing maps of titanium alloys in isothermal compression, Materials Science and Engineering: A, Vol. 504, 2009, pp. 90-98.

[10] FORBES JONES R.M., JACKMAN L.A.: The structural evolution of superalloy ingots during hot working. JOM, Vol. 51, No. 1, 1999, pp. 27-31.

[11] A. ŚWIĄTONIOWSKI (ed.), Modification of the composition of superalloys based on nickel and chromium by deformation in the rolling process, AGH, Kraków: ARBOR FP, 2013.

[12] MURTY S.V.S.N., RAO B.N. Ziegler's Criterion on the Instability Regions in Processing Maps. Journal of Materials Science Letters, Vol. 17, No. 14, 1998, pp. 1203-1205.

[13] WEN D., LIN Y.C., LI H., CHEN X., DENG J., LI L. Hot deformation behavior and processing map of a typical Ni-based superalloy. Materials Science and Engineering: A, Vol. 591, 2014, pp.183-192.

[14] QForm manual.